Hindawi
Mathematical Problems in Engineering
Volume 2021, Article ID 8740634, 9 pages
https://doi.org/10.1155/2021/8740634

*Research Article*

# An Efficient Finite Element Method and Error Analysis for Schrödinger Equation with Inverse Square Singular Potential

**Hui Zhang**,[1] **Fubiao Lin**,[2] **and Junying Cao**[3]

[1]*Guizhou Key Laboratory of Information and Computing Sciences, Guizhou Normal University, Guiyang, Guizhou 550025, China*
[2]*Department of Mathematics and Statistics, Guizhou University of Finance and Economics, Guiyang, Guizhou 550025, China*
[3]*School of Data Science and Information Engineering, Guizhou Minzu University, Guiyang 550025, China*

Correspondence should be addressed to Junying Cao; caojunying@gzmu.edu.cn

Received 21 April 2021; Revised 15 May 2021; Accepted 2 June 2021; Published 14 June 2021

Academic Editor: Ruben Specogna

Copyright © 2021 Hui Zhang et al. This is an open access article distributed under the Creative Commons Attribution License, which permits unrestricted use, distribution, and reproduction in any medium, provided the original work is properly cited.

We provide in this study an effective finite element method of the Schrödinger equation with inverse square singular potential on circular domain. By introducing proper polar condition and weighted Sobolev space, we overcome the difficulty of singularity caused by polar coordinates' transformation and singular potential, and the weak form and the corresponding discrete scheme based on the dimension reduction scheme are established. Then, using the approximation properties of the interpolation operator, we prove the error estimates of approximation solutions. Finally, we give a large number of numerical examples, and the numerical results show the effectiveness of the algorithm and the correctness of the theoretical results.

## 1. Introduction

Schrödinger equation with the inverse square or centrifugal potential plays an important role in quantum mechanics, quantum cosmology, nuclear physics, molecular physics, and so on [1–8]. The potential has the same differential order as the Laplacian operator near the origin, which usually leads to strong singularities and cannot be treated as a lower-order perturbation term [9–14]. Li et al. [15] proposed an efficient finite element method to discuss the numerical solution of time-fractional Schrö dinger equations. Thus, we need to develop some new numerical methods to solve Schrödinger equation with inverse square singular potential.

In recent years, more and more attention has been paid to the numerical methods of the schrödinger equations with similar singular potential [1, 16–21]. However, many numerical methods are based on low-order finite element methods. If we solve these problems directly in two-dimensional domain, it will cost a lot of computing time and memory capacity to obtain high-precision numerical solutions [22–24]. In practice, we usually need to solve the Schrödinger equation with inverse square singular potential on circular domain. As far as we know, there are few reports on an effective numerical method for the Schrödinger equation with inverse square potential in circular domain. Thus, the purpose of this paper is to propose an effective finite element method of the Schrödinger equation with inverse square singular potential on circular domain. By introducing proper polar condition and weighted Sobolev space, we overcome the difficulty of singularity caused by polar coordinates transformation and singular potential and establish the weak form and corresponding discrete scheme based on the dimension reduction format. Then, using the approximation properties of interpolation operator, we prove the error estimates of approximation solutions. Finally, we give a large number of numerical examples, and the numerical results show the effectiveness of the algorithm and the correctness of the theoretical results [25, 26].

The rest of this paper is organized as follows. In Section 2, we derive an equivalent scheme based on variable separation. In Section 3, we prove the existence and uniqueness of the solution. In Section 4, we prove the error estimation of approximation solutions. In Section 5, we describe the details for an efficient implementation of the algorithm. In

Section 6, we provide some numerical experiments to show the accuracy and efficiency of our algorithm. Finally, in Section 7, we give some concluding remarks.

## 2. An Equivalent Scheme Based on Variable Separation

We are interested in studying the following Schrödinger equation with inverse square singular potential:

$$-\Delta\psi(x,y)+\frac{\beta(r)}{r^2}\psi(x,y)=f(x,y),\quad \text{in } D, \tag{1}$$

$$\psi(x,y)=0,\quad \text{on } \partial D, \tag{2}$$

where $0<\beta_*\le\beta(r)\le\beta^*$ and $D=\{x\in\mathbb{R}^2\colon 0\le r<R\}$ with $r=\sqrt{x^2+y^2}$. Let $x=r\cos\theta$, $y=r\sin\theta$, $U(r,\theta)=\psi(x,y)$, and $F(r,\theta)=f(x,y)$. Then, the Laplace operator in polar coordinates is as follows:

$$\mathscr{L}U=\frac{1}{r}\frac{\partial}{\partial r}\left(r\frac{\partial U}{\partial r}\right)+\frac{1}{r^2}U_{\theta\theta}. \tag{3}$$

We can rewrite (1) and (2) as follows:

$$-r\mathscr{L}U(r,\theta)+\frac{\beta(r)}{r}U(r,\theta)=rF(r,\theta),\ (r,\theta)\in(0,R)\times[0,2\pi], \tag{4}$$

$$U(R,\theta)=0. \tag{5}$$

Since $U(r,\theta)$ and $F(r,\theta)$ are $2\pi$ periodic in $\theta$, then we have

$$\begin{aligned} U(r,\theta)&=\sum_{|m|=0}^{\infty}u_m(r)e^{im\theta},\\ F(r,\theta)&=\sum_{|m|=0}^{\infty}f_m(r)e^{im\theta}, \end{aligned} \tag{6}$$

where $u_m$ and $f_m$ are the Fourier coefficients of $U(r,\theta)$ and $F(r,\theta)$, respectively. We can derive from (3) and (6) that

$$r\mathscr{L}U(r,\theta)=\sum_{|m|=0}^{\infty}\left[\frac{\partial}{\partial r}\left(r\frac{\partial u_m(r)}{\partial r}\right)-\frac{m^2}{r}u_m(r)\right]e^{im\theta}, \tag{7}$$

$$\frac{U(r,\theta)}{r}=\sum_{|m|=0}^{\infty}\frac{u_m(r)}{r}e^{im\theta}. \tag{8}$$

To make (7) and (8) meaningful, we need introduce the following essential pole conditions:

$$m^2u_m(0)=0,\quad u_m(0)=0. \tag{9}$$

The pole condition (9) can be further reduced to

$$u_m(0)=0. \tag{10}$$

Using the orthogonal properties of Fourier basis functions and polar condition (10), we can reduce (4) and (5) to a series of equivalent one-dimensional Schrödinger equations as follows:

$$-r\mathscr{L}_m u_m(r)+\frac{\beta(r)}{r}u_m(r)=rf_m(r),\quad r\in(0,R), \tag{11}$$

$$u_m(0)=u_m(R)=0, \tag{12}$$

where

$$\mathscr{L}u_m(r)=\frac{1}{r}\frac{\partial}{\partial r}\left(r\frac{\partial u_m(r)}{\partial r}\right)-\frac{m^2}{r^2}u_m(r). \tag{13}$$

## 3. Existence and Uniqueness of the Solution

For convenience, we use the expression $a\lesssim b$ to mean that $a\le Cb$, where $C$ is a positive constant. In order to derive the weak form and corresponding discrete scheme of equations (11) and (12), we need to introduce the usual weighted Sobolev space:

$$L^2_\omega(0,R):=\left\{u\colon \int_0^R\omega u^2\mathrm{d}r<\infty\right\}, \tag{14}$$

with the corresponding inner product and norm,

$$\begin{aligned} (u,v)_\omega&=\int_0^R\omega uv\,\mathrm{d}r,\\ \|u\|_w&=\left(\int_0^R\omega u^2\mathrm{d}r\right)^{1/2}, \end{aligned} \tag{15}$$

and the nonuniformly weighted Sobolev space:

$$\begin{aligned} \mathscr{H}^1_{0,\omega}(0,R):=\{&u_m\colon \partial_r^k u_m\in L^2_{\omega^{2k-1}}(0,R),\\ &k=0,1,u_m(0)=u_m(R)=0\}, \end{aligned} \tag{16}$$

with the corresponding inner product and norm,

$$\begin{aligned} (u_m,v_m)_{1,\omega}&=\int_0^R r\partial_r u_m\partial_r v_m+\frac{1}{r}u_mv_m\mathrm{d}r,\\ \|u_m\|_{1,\omega}&=(u_m,u_m)^{1/2}_{1,\omega}, \end{aligned} \tag{17}$$

where $\omega=r$ is a weight function. Then, the weak form of equations (11) and (12) is to find $u_m\in\mathscr{H}^1_{0,\omega}(0,R)$, such that

$$a_m(u_m,v_m)=F_m(v_m),\quad \forall v_m\in\mathscr{H}^1_{0,\omega}(0,R), \tag{18}$$

where

$$\begin{aligned} a_m(u_m,v_m)&=\int_0^R r\partial_r u_m\partial_r v_m+\frac{m^2+\beta(r)}{r}u_mv_m\mathrm{d}r,\\ F_m(v_m)&=\int_0^R rf_mv_m\mathrm{d}r. \end{aligned} \tag{19}$$

Define approximation space $X_h=P_h\cap\mathscr{H}^1_{0,\omega}(0,R)$, where $P_h$ is a piecewise linear interpolation polynomial space. Then, the corresponding discrete scheme of (18) is to find $u_{mh}\in X_h$, such that

$$a_m(u_{mh},v_{mh})=F_m(v_{mh}),\quad \forall v_{mh}\in X_h. \tag{20}$$

**Lemma 1.** *$a_m(u_m, v_m)$ is a continuous and coercive bilinear functional on $\mathscr{H}^1_{0,\omega}(0,R) \times \mathscr{H}^1_{0,\omega}(0,R)$, i.e.,*

$$\begin{aligned} |a_m(u_m, v_m)| &\lesssim \|u_m\|_{1,\omega}\|v_m\|_{1,\omega}, \\ a_m(u_m, u_m) &> \mathrm{rsim}\|u_m\|^2_{1,\omega}. \end{aligned} \tag{21}$$

*Proof.* We derive from the Cauchy–Schwarz inequality that

$$\begin{aligned} |a_m(u_m, v_m)| &= \left|\int_0^R r\partial_r u_m \partial_r v_m + \frac{m^2+\beta(r)}{r} u_m v_m \mathrm{d}r\right| \\ &\le \int_0^R r\partial_r |u_m \partial_r v_m| + \frac{m^2+\beta^*}{r}|u_m v_m| \mathrm{d}r \\ &\lesssim \int_0^R r\partial_r |u_m \partial_r v_m| + \frac{1}{r}|u_m v_m| \mathrm{d}r \\ &\lesssim \left(\int_0^R r|\partial_r u_m|^2 \mathrm{d}r\right)^{1/2}\left(\int_0^R r|\partial_r v_m|^2 \mathrm{d}r\right)^{1/2} \\ &\quad + \left(\int_0^R \frac{1}{r}|u_m|^2 \mathrm{d}r\right)^{1/2}\left(\int_0^R \frac{1}{r}|v_m|^2 \mathrm{d}r\right)^{1/2} \\ &\lesssim \left(\int_0^R r|\partial_r u_m|^2 + \frac{1}{r}|u_m|^2 \mathrm{d}r\right)^{1/2} \\ &\quad \left(\int_0^R r|\partial_r v_m|^2 + \frac{1}{r}|v_m|^2 \mathrm{d}r\right)^{1/2} \\ &\lesssim \|u_m\|_{1,\omega}\|v_m\|_{1,\omega}, \\ a_m(u_m, u_m) &= \int_0^R r(\partial_r u_m)^2 + \frac{m^2+\beta(r)}{r}(u_m)^2 \mathrm{d}r \\ &\ge \int_0^R r(\partial_r u_m)^2 + \frac{m^2+\beta_*}{r}(u_m)^2 \mathrm{d}r \\ &\lesssim \int_0^R r(\partial_r u_m)^2 + \frac{1}{r}(u_m)^2 \mathrm{d}r \lesssim \|u_m\|^2_{1,\omega}. \end{aligned} \tag{22}$$

**Lemma 2.** *If $f_m \in L^2_\omega(0,R)$, then $F_m(v_m)$ is a bounded linear functional on $\mathscr{H}^1_{0,\omega}(0,R)$, i.e.,*

$$|F_m(v_m)| \lesssim \|u_m\|_{1,\omega}. \tag{23}$$

*Proof.* From Cauchy–Schwarz inequality, we have

$$\begin{aligned} |F_m(v_m)| &= \left|\int_0^R r f_m v_m \mathrm{d}r\right| \lesssim \left[\int_0^R r(f_m)^2 \mathrm{d}r\right]^{1/2}\left[\int_0^R r(v_m)^2 \mathrm{d}r\right]^{1/2} \\ &\lesssim \|f_m\|_\omega \left[\int_0^R r(\partial_r u_m)^2 + \frac{R^2}{r}(v_m)^2 \mathrm{d}r\right]^{1/2} \lesssim \|u_m\|_{1,\omega}. \end{aligned} \tag{24}$$

□

This finishes our proof.

**Theorem 1.** *If $f_m \in L^2_\omega(0,R)$, then problems (18) and (20) have unique solutions $u_m$ and $u_{mh}$, respectively.*

*Proof.* From Lemma 1, we have

$$\begin{aligned} |a_m(u_m, v_m)| &\lesssim \|u_m\|_{1,\omega}\|v_m\|_{1,\omega}, \\ a_m(u_m, u_m) &\lesssim \|u_m\|^2_{1,\omega}, \end{aligned} \tag{25}$$

for $\forall u_m, v_m \in \mathscr{H}^1_{0,\omega}(0,R)$. That is, $a_m(u_m, v_m)$ is a bounded and positive definite bilinear functional defined on $\mathscr{H}^1_{0,\omega}(0,R) \times \mathscr{H}^1_{0,\omega}(0,R)$. In addition, from Lemma 2, we have

$$|F_m(v_m)| \lesssim \|u_m\|_{1,\omega}, \tag{26}$$

which means $F_m(v_m)$ is a bounded linear functional defined on $\mathscr{H}^1_{0,\omega}(0,R)$. Then, from Lax–Milgram lemma, we know that equations (18) and (20) have unique solutions $u_m$ and $u_{mh}$, respectively. □

## 4. Error Estimation of Approximation Solutions

In this section, we will present the error estimates of approximate solutions. Define the piecewise linear interpolation operator $\mathscr{I}_h$: $\mathscr{H}^1_{0,\omega}(0,R) \longrightarrow X_h$ by

$$\mathscr{I}_h u_m(r) = p_{mi}(r), \quad r \in I_i, \tag{27}$$

where $p_{mi}(r)$ is the linear interpolation polynomial of $u_m$ on interval $I_i = [r_{i-1}, r]_i$. Let

$$u_{mi}(r) = u_m(r), \quad r \in I_i. \tag{28}$$

Then, from error formula of linear interpolating remainder term, we have

$$u_{mi}(r) - p_{mi}(r) = \frac{\partial_r^2 u_{mi}(\xi_i)}{2!}(r - r_{i-1})(r - r_i), \tag{29}$$

where $\xi_i \in I_i$ is a function depending on $r$.

**Theorem 2.** *Let $G_{mi}(r) = \partial_r^2 u_{mi}(\xi_i)/2!$. Suppose that $u_m$ is smooth enough such that $|\partial_r^k G_{mi}(r)| \le M$ $(k = 0, 1)$, where $M$ is a large enough constant$(0 \le m \le M)$ in Fourier transformation. Then, it holds*

$$\int_0^R [\partial_r(\mathscr{I}_h u_m(r) - u_m(r))]^2 \mathrm{d}r \lesssim h^2, \tag{30}$$

*where $h = \max_{1\le i\le n}\{h_i\}$, $h_i = r_i - r_{i-1}$.*

*Proof.* Since

$$\begin{aligned} u_{mi}(r) - \mathscr{I}_h u_{mi}(r) &= u_{mi}(r) - p_{mi}(r) \\ &= G_{mi}(r)(r - r_{i-1})(r - r_i), \end{aligned} \tag{31}$$

then we derive that

$$\partial_r\left(u_{mi}(r)-\mathcal{I}_h u_{mi}(r)\right)=\partial_r G_{mi}(r)(r-r_{i-1})(r-r_i)+G_{mi}(r)\partial_r\left((r-r_{i-1})(r-r)_i\right). \tag{32}$$

Then, we obtain

$$\begin{aligned}\left|\partial_r\left(u_{mi}(r)-\mathcal{I}_h u_{mi}(r)\right)\right|^2 &\lesssim \left|(r-r_{i-1})(r-r_i)\right|^2\\ &\quad+\left|\partial_r\left((r-r_{i-1})(r-r_i)\right)\right|^2\\ &=\left|(r-r_{i-1})(r-r_i)\right|^2\\ &\quad+\left|(r-r_i)+(r-r_{i-1})\right|^2\\ &\le\left(\frac{h_i}{2}\right)^4+(2h_i)^2\\ &\lesssim h_i^2.\end{aligned} \tag{33}$$

Thus, we derive that

$$\begin{aligned}&\int_0^R\left[\partial_r\left(\mathcal{I}_h u_m(r)-u_m(r)\right)\right]^2\mathrm{d}r\\ &=\sum_{i=1}^n\int_{r_{i-1}}^{r_i}\left[\partial_r\left(\mathcal{I}_h u_{mi}(r)-u_{mi}(r)\right)\right]^2\mathrm{d}r\\ &\lesssim\sum_{i=1}^n h_i^3\\ &\lesssim h^2.\end{aligned} \tag{34}$$

□

The proof of Theorem 2 is complete.

**Lemma 3.** *For any $u_m(r)\in\mathcal{H}^1_{0,\omega}(0,R)$, the following inequality holds:*

$$\int_0^R\frac{1}{r}u_m^2(r)\mathrm{d}r\le R\int_0^R\left(\partial_r u_m(r)\right)^2\mathrm{d}r. \tag{35}$$

*Proof.* Since $u_m(r)\in\mathcal{H}^1_{0,\omega}(0,R)$, then we have

$$\begin{aligned}\frac{1}{r}u_m^2(r)&=\frac{1}{r}\left(\int_0^r\partial_r u_m(t)\mathrm{d}t\right)^2\le\frac{1}{r}\int_0^r 1^2\mathrm{d}t\int_0^r\left(\partial_r u_m(t)\right)^2\mathrm{d}t\\ &=\int_0^r\left(\partial_r u_m(t)\right)^2\mathrm{d}t\le\int_0^R\left(\partial_r u_m(r)\right)^2\mathrm{d}r.\end{aligned} \tag{36}$$

Thus, we derive that

$$\int_0^R\frac{1}{r}u_m^2(r)\,\mathrm{d}r\le R\int_0^R\left(\partial_r u_m(r)\right)^2\mathrm{d}r. \tag{37}$$

□

**Theorem 3.** *Let $u_m$ and $u_{mh}$ be the solutions of problems (18) and (20), respectively. Then, the following inequality holds:*

$$\left\|u_m-u_{mh}\right\|_{1,\omega}\lesssim h. \tag{38}$$

*Proof.* We derive from (18) and (20) that

$$\begin{aligned}a_m(u_m,v_{mh})&=F_m(v_{mh}),\quad\forall v_{mh}\in X_h,\\ a_m(u_{mh},v_{mh})&=F_m(v_{mh}),\quad\forall v_{mh}\in X_h.\end{aligned} \tag{39}$$

Then, we have

$$a_m(u_m-u_{mh},v_{mh})=0,\quad\forall v_{mh}\in X_h. \tag{40}$$

We derive from Lemma 1 and (40) that

$$\begin{aligned}\left\|u_m-u_{mh}\right\|_{1,\omega}^2&\lesssim a_m(u_m-u_{mh},u_m-u_{mh})\\ &=a_m(u_m-u_{mh},u_m-v_{mh}+v_{mh}-u_{mh})\\ &=a_m(u_m-u_{mh},u_m-v_{mh})\\ &\lesssim\left\|u_m(r)-u_{mh}\right\|_{1,\omega}\left\|u_m-v_{mh}\right\|_{1,\omega}.\end{aligned} \tag{41}$$

Then, we obtain

$$\left\|u_m-u_{mh}\right\|_{1,\omega}\lesssim\left\|u_m-v_{mh}\right\|_{1,\omega},\quad\forall v_{mh}\in X_h. \tag{42}$$

Then, we have

$$\begin{aligned}\left\|u_m-u_{mh}\right\|_{1,\omega}^2&\lesssim\inf_{v_{mh}\in X_N}\left\|u_m-v_{mh}\right\|_{1,\omega}^2\lesssim\left\|u_m-\mathcal{I}_h u_m\right\|_{1,\omega}^2\\ &=\int_0^R r\left[\partial_r\left(u_m-\mathcal{I}_h u_m\right)\right]^2+\frac{1}{r}\left(u_m-\mathcal{I}_h u_m\right)^2\mathrm{d}r.\end{aligned} \tag{43}$$

We derive from Lemma 3 that

$$\begin{aligned}\left\|u_m-u_{mh}\right\|_{1,\omega}^2&\lesssim\int_0^R r\left[\partial_r\left(u_m-\mathcal{I}_h u_m\right)\right]^2+\frac{1}{r}\left(u_m-\mathcal{I}_h u_m\right)^2\mathrm{d}r\\ &\lesssim\int_0^R R\left[\partial_r\left(u_m-\mathcal{I}_h u_m\right)\right]^2\mathrm{d}r\lesssim\int_0^R\left[\partial_r\left(u_m-\mathcal{I}_h u_m\right)\right]^2\mathrm{d}r.\end{aligned} \tag{44}$$

Combining with Theorem 2, we can obtain the desired result. □

## 5. Implementation of the Algorithm

To solve the discrete scheme (20), we need to construct a set of basis functions of approximation space. Let

$$\psi_i(r)=\begin{cases}\dfrac{r-r_{i-1}}{h_i}, & r_{i-1}\le r\le r_i,\\[2ex] -\dfrac{r-r_{i+1}}{h_{i+1}}, & r_i\le r\le r_{i+1},\\[2ex] 0, & \text{others},\end{cases} \tag{45}$$

where $i=1,\ldots,N-1$. It is clear that

$$X_h = \operatorname{span}\{\psi_1(r), \ldots, \psi_{N-1}(r)\}. \tag{46}$$

Set

$$\begin{aligned} a_{ij} &= \int_0^R r\left(\psi_j(r)\right)'\left(\psi_i(r)\right)' \mathrm{d}r, \\ b_{ij} &= \int_0^R \frac{1}{r}\psi_j(r)\psi_i(r)\,\mathrm{d}r, \\ c_{ij} &= \int_0^R \frac{\beta(r)}{r}\psi_j(r)\psi_i(r)\mathrm{d}r, \\ f_j &= \int_0^R r f_m(r)\psi_j(r)\mathrm{d}r. \end{aligned} \tag{47}$$

Let

$$u_{mh} = \sum_{k=1}^{N-1} u_m^k \psi_k(r). \tag{48}$$

Substituting expression (48) into (20) and taking $v_{mh}$ through all the basis functions in $X_h$, we obtain the following linear system:

$$\left(\mathbb{A} + m^2\mathbb{B} + \mathbb{C}\right)\mathbb{U} = \mathbb{F}, \tag{49}$$

where

$$\begin{aligned} \mathbb{A} &= \left(a_{ij}\right), \\ \mathbb{B} &= \left(b_{ij}\right), \\ \mathbb{C} &= \left(c_{ij}\right), \\ \mathbb{F} &= \left(f_1, \ldots, f_{N-1}\right)^T, \\ \mathbb{U} &= \left(u_1, \ldots, u_{N-1}\right)^T. \end{aligned} \tag{50}$$

From the properties of the basis functions, we know that the stiff matrices and mass matrix in (49) are all tridiagonal sparse matrices.

## 6. Numerical Experiments

We will perform some numerical tests in order to show the convergence and the effectiveness of our algorithm. We operate our programs in MATLAB 2015b.

Let $\psi_{Mh}(x, y)$ be the approximation solution of exact solution $\psi(x, y)$.

By using the following polar coordinate transformation,

$$\begin{aligned} x &= r\cos\theta, \\ y &= r\sin\theta, \quad (0 \le r \le R, 0 \le \theta < 2\pi), \end{aligned} \tag{51}$$

we obtain

$$\begin{aligned} \psi(x, y) = U(r, \theta) &= \sum_{|m|=0}^{\infty} u_m(r)e^{im\theta}, \\ \psi_{Mh}(x, y) = U_{Mh}(r, \theta) &= \sum_{|m|=0}^{M} u_{mh}(r)e^{im\theta}. \end{aligned} \tag{52}$$

We define the error between the exact solution $\psi(x, y)$ and the approximation solution $\psi_{Mh}(x, y)$ as follows:

$$\begin{aligned} e\left(\psi(x, y), \psi_{Mh}(x, y)\right) &= \left\|\psi(x, y) - \psi_{Mh}(x, y)\right\|_{L^\infty(D)} \\ &= \left\|U(r, \theta) - U_{Mh}(r, \theta)\right\|_{L^\infty(\mathscr{D})}. \end{aligned} \tag{53}$$

*Example 1.* We take $\beta(r) = r^2 + 4, R = 1, \psi(x, y) = xy(x^2 + y^2 - 1)$. It is clear that $\psi(x, y)$ satisfies the boundary condition (2). The $f(x, y)$ can be obtained by substituting $\psi(x, y)$ into equation (1). Next, we solve problems (1) and (2) by using the algorithm proposed in this paper. We list the errors between exact solution and approximation solutions in Table 1 for different $M$ and $h$. In order to further show the accuracy and convergence of our algorithm, we present the figures and their error figures of exact solution and approximation solution in Figures 1 and 2, respectively.

We observe from Table 1 that the error $e(\psi(x, y), \psi_{Mh}(x, y))$ achieve about $10^{-4}$ with $h \le (1/32)$ and $M = 6$. In addition, we can see from Figures 1 and 2 that the numerical solution converges to exact solution with the decrease of $h$.

*Example 2.* We take $\beta(r) = (2/3), R = 1$, and $u = (x^2 + y^2 - 1)\sin(x^2 + y^2)$. It is obvious that $\psi(x, y)$ satisfies the boundary condition (2). Similarly, $f(x, y)$ can be obtained by substituting $\psi(x, y)$ into equation (1). We list the errors between exact solution and approximation solutions in Table 2 for different $M$ and $h$. In order to further show the accuracy and convergence of our algorithm, we present the figures and their error figures of exact solution and approximation solution in Figures 3 and 4, respectively.

We observe from Table 2 that the error $e(\psi(x, y), \psi_{Mh}(x, y))$ achieves about $10^{-4}$ with $h \le (1/32)$ and $M = 6$. In addition, we can see from Figures 3 and 4 that the numerical solution converges to exact solution with the decrease of $h$.

*Example 3.* We take $\beta = 1/2, R = 1$, and $\psi(x, y) = (x^2 + y^2 - 1)xe^{x+y}$. We list the errors between exact solution and approximation solutions in Table 3 for different $M$ and $h$. We also present the figures and their error figures of exact solution and approximation solution in Figures 5 and 6, respectively.

Table 1: The error $e(\psi(x,y), \psi_{Mh}(x,y))$ for different $M$ and $h$.

| $h$ | $M = 6$ | $M = 8$ | $M = 10$ | $M = 12$ |
|---|---|---|---|---|
| 1/8 | 0.0517 | 0.0517 | 0.0754 | 0.0754 |
| 1/16 | $4.4437e-04$ | $4.4437e-04$ | $4.4437e-04$ | $4.4437e-04$ |
| 1/32 | $1.1380e-04$ | $1.1380e-04$ | $1.1380e-04$ | $1.1380e-04$ |
| 1/64 | $2.8623e-05$ | $2.8623e-05$ | $2.8623e-05$ | $2.8623e-05$ |

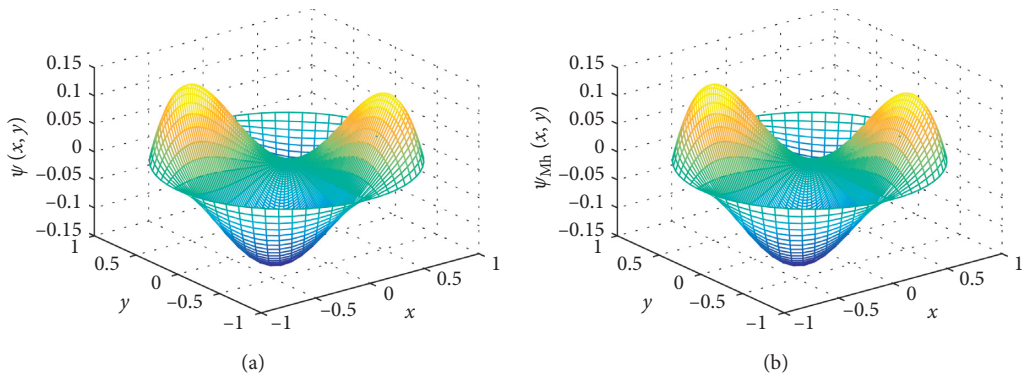


Figure 1: Figures of the exact solution (a) and the numerical solution (b) with $h = 1/64, m = 12$.

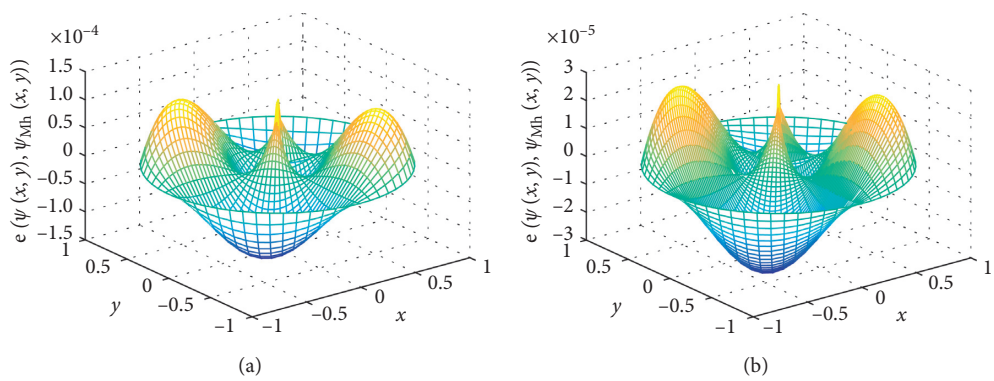


Figure 2: The error figures of exact solution and numerical solution with $h = 1/32, m = 10$ (a) and $h = 1/64, m = 12$ (b).

Table 2: The error $e(\psi(x,y), \psi_{Mh}(x,y))$ for different $M$ and $h$.

| $h$ | $M = 6$ | $M = 8$ | $M = 10$ | $M = 12$ |
|---|---|---|---|---|
| 1/8 | 0.0027 | 0.0978 | 0.0978 | 0.0978 |
| 1/16 | $6.5774e-04$ | $6.5774e-04$ | $6.5774e-04$ | $6.5774e-04$ |
| 1/32 | $1.6360e-04$ | $1.6360e-04$ | $1.6360e-04$ | $1.6360e-04$ |
| 1/64 | $4.0798e-05$ | $4.0798e-05$ | $4.0798e-05$ | $4.0798e-05$ |

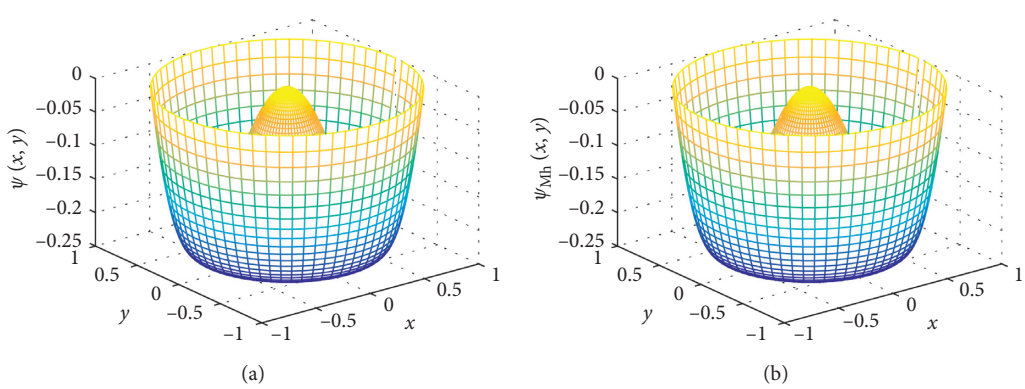


Figure 3: Figures of the exact solution (a) and the numerical solution (b) with $h = 1/64, m = 12$.

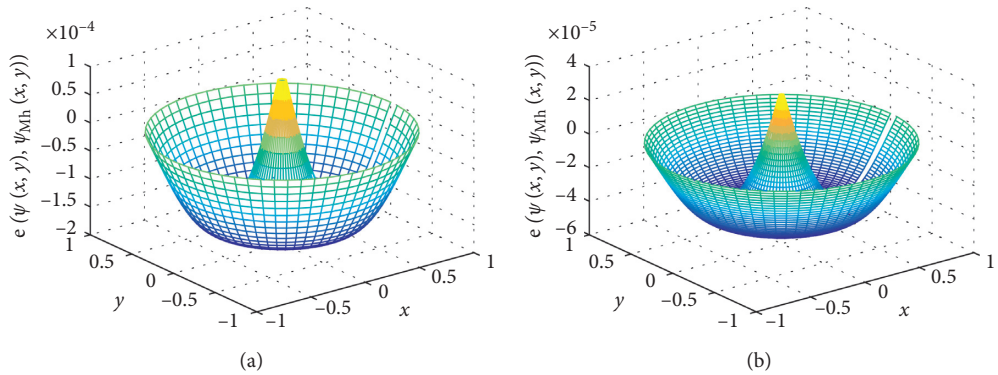


Figure 4: The error figures of numerical solution and exact solution with $h = 1/32, m = 10$ (a) and $h = 1/64, m = 12$ (b).

Table 3: The error $e(\psi(x, y), \psi_{Mh}(x, y))$ for different $M$ and $h$.

| $h$ | $M = 6$ | $M = 8$ | $M = 10$ | $M = 12$ |
|---|---|---|---|---|
| 1/16 | 0.0022 | 0.0022 | 0.0022 | 0.0050 |
| 1/32 | $5.4324e-04$ | $5.4324e-04$ | $5.4324e-04$ | $5.4324e-04$ |
| 1/64 | $1.3583e-04$ | $1.3583e-04$ | $1.3583e-04$ | $1.3583e-04$ |
| 1/128 | $4.1754e-05$ | $3.3967e-05$ | $3.3944e-05$ | $3.3944e-05$ |

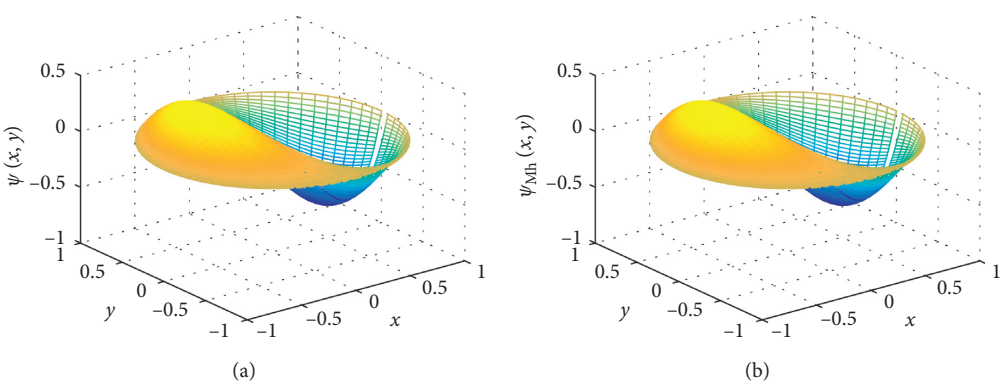


Figure 5: Figures of the exact solution (a) and the numerical solution (b) with $h = 1/128, m = 12$.

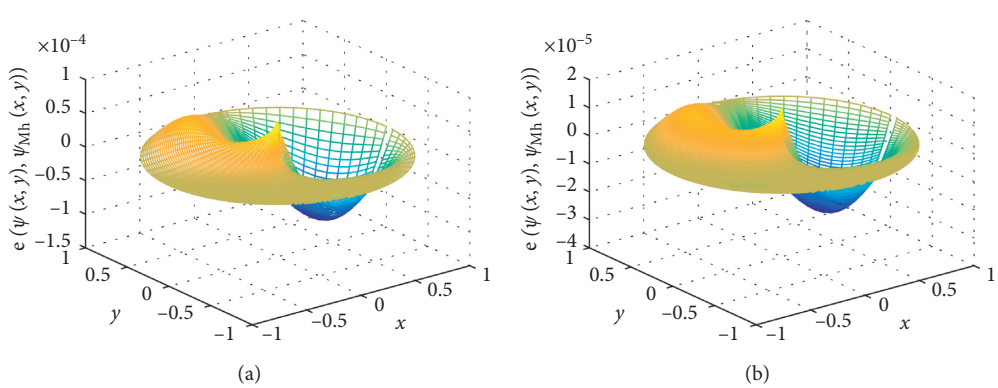


Figure 6: The error figures of numerical solution and exact solution with $h = 1/64, m = 10$ (a) and $h = 1/128, m = 12$ (b).

We observe from Table 3 that the error $e(\psi(x, y), \psi_{Mh}(x, y))$ achieves about $10^{-4}$ with $h \leq (1/64)$ and $M = 6$. In addition, we can see from Figures 5 and 6 that the numerical solution converges to exact solution with the decrease of $h$.

## 7. Conclusions

We present in this paper an efficient finite element method for the Schrödinger equation with the inverse square potential on the circular domain. By using polar coordinate transformation and Fourier basis function expansion, we reduce the original problem into a series of equivalent one-dimensional problems. By introducing polar conditions, we overcome not only the difficulty brought by the singular potential but also the degree of freedom which is greatly reduced by dimension reduction. Thus, we only spend less computing time and memory capacity to obtain high-precision numerical solutions. Numerical results show that our algorithm is very effective. We mainly focus on, in this paper, the Schrödinger equation with the inverse square potential on the circular domain. In fact, we can extend our method to the Schrödinger equation with more complex potentials.

## Data Availability

The data used to support the findings of this study are included within the article.

## Conflicts of Interest

The authors declare that they have no conflicts of interest.

## Acknowledgments

The research of Junying Cao was supported by NSFC (nos. 11901135 and 11961009) and Foundation of Guizhou Science and Technology Department (nos. [2020]1Y015 and [2017]1086).

## References

[1] V. Felli, E. Marchini, E. M. Marchini, and S. Terracini, "On the behavior of solutions to Schrödinger equations with dipole type potentials near the singularity," *Discrete & Continuous Dynamical Systems-A*, vol. 21, no. 1, pp. 91–119, 2008.

[2] S. Fournais, M. Hoffmann-Ostenhof, T. Hoffmann-Ostenhof, and T. Ø. Sørensen, "Analytic structure of solutions to multiconfiguration equations," *Journal of Physics A: Mathematical and Theoretical*, vol. 42, no. 31, Article ID 315208, 2009.

[3] S. Moroz and R. Schmidt, "Nonrelativistic inverse square potential, scale anomaly, and complex extension," *Annals of Physics*, vol. 325, no. 2, pp. 491–513, 2010.

[4] H. Wu and D. W. L. Sprung, "Inverse-square potential and the quantum vortex," *Physical Review A*, vol. 49, no. 6, pp. 4305–4311, 1994.

[5] K. M. Case, "Singular potentials," *Physical Review*, vol. 80, no. 5, pp. 797–806, 1950.

[6] W. M. Frank, D. J. Land, and R. M. Spector, "Singular potentials," *Reviews of Modern Physics*, vol. 43, no. 1, pp. 36–98, 1971.

[7] J. Zhang and X. Yang, "Decoupled, non-iterative, and unconditionally energy stable large time stepping method for the three-phase Cahn-Hilliard phase-field model," *Journal of Computational Physics*, vol. 404, Article ID 109115, 2020.

[8] J. Zhang and X. Yang, "Unconditionally energy stable large time stepping method for the L2-gradient flow based ternary phase-field model with precise nonlocal volume conservation," *Computer Methods in Applied Mechanics and Engineering*, vol. 361, Article ID 112743, 2020.

[9] D. Cao and P. Han, "Solutions to critical elliptic equations with multi-singular inverse square potentials," *Journal of Differential Equations*, vol. 224, no. 2, pp. 332–372, 2006.

[10] V. Felli, E. M. Marchini, and S. Terracini, "On Schrödinger operators with multipolar inverse-square potentials," *Journal of Functional Analysis*, vol. 250, no. 2, pp. 265–316, 2007.

[11] V. Felli and S. Terracini, "Elliptic equations with multi-singular inverse-square potentials and critical nonlinearity," *Communications in Partial Differential Equations*, vol. 31, no. 3, pp. 469–495, 2006.

[12] H. Kalf, U.-W. Schmincke, J. Walter, and R. Wüst, "On the spectral theory of Schrödinger and Dirac operators with strongly singular potentials," in *Spectral Theory and Differential Equations*, pp. 182–226, Springer, Berlin, Germany, 1975.

[13] J. Zhang and X. Yang, "A fully decoupled, linear and unconditionally energy stable numerical Scheme for a melt-convective phase-field dendritic solidification model," *Computer Methods in Applied Mechanics and Engineering*, vol. 363, Article ID 112779, 2020.

[14] J. Zhang, C. Chen, X. Yang, Y. Chu, and Z. Xia, "Efficient, Non-iterative, and second-order accurate numerical algorithms for the anisotropic Allen-Cahn Equation with precise nonlocal mass conservation," *Journal of Computational and Applied Mathematics*, vol. 363, pp. 444–463, 2020.

[15] D. Li, J. Wang, and J. Zhang, "Unconditionally convergent $L1$-Galerkin FEMs for nonlinear time-fractional schrödinger equations," *SIAM Journal on Scientific Computing*, vol. 39, no. 6, pp. A3067–A3088, 2017.

[16] V. Felli, A. Ferrero, and S. Terracini, "Asymptotic behavior of solutions to Schrödinger equations near an isolated singularity of the electromagnetic potential," *Journal of the European Mathematical Society*, vol. 13, pp. 119–174, 2011.

[17] E. Hunsicker, H. Li, V. Nistor, and U. Ville, "Analysis of Schrodinger operators with inverse square potentials I: regularity results in 3D," *Bulletin Mathématique de laSociété des Sciences*, vol. 55, pp. 157–178, 2012.

[18] H. Li and V. Nistor, "Analysis of a modified Schrödinger operator in 2D: regularity, index, and FEM," *Journal of Computational and Applied Mathematics*, vol. 224, no. 1, pp. 320–338, 2009.

[19] H. Li and Z. Zhang, "Efficient spectral and spectral element methods for eigenvalue problems of schrödinger equations with an inverse square potential," *SIAM Journal on Scientific Computing*, vol. 39, no. 1, pp. A114–A140, 2017.

[20] Y. Sui, G. Zhang, J. Cao, and J. Zhang, "An efficient finite element method and error analysis for eigenvalue problem of Schrödinger equation with an inverse square potential on spherical domain," *Advances in Difference Equations*, vol. 1, pp. 1–15, 2020.

[21] L. Li and J. An, "An efficient spectral method and rigorous error analysis based on dimension reduction scheme for fourth order problems," *Numerical Methods for Partial Differential Equations*, vol. 37, no. 2021, pp. 152–171.

[22] H. Li and J. S. Ovall, "A posteriori error estimation of hierarchical type for the Schrödinger operator with inverse square potential," *Numerische Mathematik*, vol. 128, no. 4, pp. 707–740, 2014.
[23] H. Li and J. S. Ovall, "A posteriori eigenvalue error estimation for a Schrödinger operator with inverse square potential," *Discrete and Continuous Dynamical Systems-Series B*, vol. 20, no. 5, pp. 1377–1391, 2015.
[24] G. W. Reddien, "Finite-difference approximations to singular Sturm-Liouville eigenvalue problems," *Mathematics of Computation*, vol. 30, no. 134, p. 278, 1976.
[25] L. Ma, J. Shen, and L. L. Wang, "Spectral approximation of time-harmonic Maxwell equations in three-dimensional exterior domains," *International Journal of Numerical Analysis and Modeling*, vol. 12, pp. 1–18, 2015.
[26] I. Babuska and J. Osborn, *Eigenvalue Problems, Handbook of Numerical Analysis*, pp. 640–787, Elsevier Science Publishers, North-Holand, Netherlands, 1991.